

D. Van Eester, E. Lerche, P. Jacquet, V. Bobkov, A. Czarnecka, J.W. Coenen,
L. Colas, K. Crombé, M. Graham, S. Jachmich, E. Joffrin, C.C. Klepperk,
V. Kiptily, M. Lehnen, C. Maggi, F. Marcotte, G. Matthews, M.-L. Mayoral,
K. Mc Cormick, I. Monakhov, M.F.F. Nave, R. Neu, C. Noble, J. Ongena,
T. Pütterich, F. Rimini, E.R. Solano, G. van Rooij
and JET EFDA contributors

Effect of the Minority Concentration on Ion Cyclotron Resonance Heating in Presence of the ITER-Like Wall in JET

Effect of the Minority Concentration on Ion Cyclotron Resonance Heating in Presence of the ITER-Like Wall in JET

D. Van Eester¹, E. Lerche¹, P. Jacquet², V. Bobkov³, A. Czarnecka⁴, J.W. Coenen⁵,
L. Colas⁶, K. Crombé¹, M. Graham¹, S. Jachmich¹, E. Joffrin⁶, C.C. Klepper⁷,
V. Kiptily¹, M. Lehnen⁵, C. Maggi³, F. Marcotte⁸, G. Matthews¹, M.-L. Mayoral¹,
K. Mc Cormick¹, I. Monakhov¹, M.F.F. Nave⁹, R. Neu³, C. Noble¹, J. Ongena¹,
T. Pütterich³, F. Rimini², E.R. Solano¹, G. van Rooij¹⁰
and JET EFDA contributors*

JET-EFDA, Culham Science Centre, OX14 3DB, Abingdon, UK

¹*LPP-ERM/KMS, Association “Euratom-Belgian State”, TEC Partner, Brussels, Belgium*

²*EURATOM-CCFE Fusion Association, Culham Science Centre, OX14 3DB, Abingdon, OXON, UK*

³*MPI für Plasmaphysik Euratom Assoziation, Garching, Germany*

⁴*Institute of Plasma Physics and Laser Microfusion, Warsaw, Poland*

⁵*IEK-4, EURATOM-FZJ, TEC Partner, Jülich, Germany*

⁶*CEA,IRFM, 13108 St-Paul-lez-Durance, France*

⁷*Oak Ridge National Laboratory, Oak Ridge, TN 37831-6169, USA*

⁸*École Nationale des Ponts et Chaussées, F77455 Marne-la-Vallée, France*

⁹*IST/IPFN Association EURATOM Lisbon, Portugal*

¹⁰*DIFFER, Assoc. EURATOM-FOM, Nieuwegein, The Netherlands*

* See annex of F. Romanelli et al, “Overview of JET Results”,
(24th IAEA Fusion Energy Conference, San Diego, USA (2012)).

Preprint of Paper to be submitted for publication in Proceedings of the
20th Topical Conference on Radio Frequency Power in Plasmas, Sorrento, Italy.

25th June 2013 - 28th June 2013

“This document is intended for publication in the open literature. It is made available on the understanding that it may not be further circulated and extracts or references may not be published prior to publication of the original when applicable, or without the consent of the Publications Officer, EFDA, Culham Science Centre, Abingdon, Oxon, OX14 3DB, UK.”

“Enquiries about Copyright and reproduction should be addressed to the Publications Officer, EFDA, Culham Science Centre, Abingdon, Oxon, OX14 3DB, UK.”

The contents of this preprint and all other JET EFDA Preprints and Conference Papers are available to view online free at www.iop.org/Jet. This site has full search facilities and e-mail alert options. The diagrams contained within the PDFs on this site are hyperlinked from the year 1996 onwards.

ABSTRACT

The most recent JET campaign has focused on characterizing operation with the “ITER-like” wall. One of the questions that needed to be answered is whether the auxiliary heating methods do not lead to unacceptably high levels of impurity influx, preventing fusion-relevant operation. In view of its high single pass absorption, hydrogen minority fundamental cyclotron heating in a deuterium plasma was chosen as the reference wave heating scheme in the ion cyclotron domain of frequencies. The present paper discusses the plasma behavior as a function of the minority concentration $X[H]$ in L-mode with up to 4MW of RF power. It was found that the tungsten concentration decreases by a factor of 4 when the minority concentration is increased from $X[H] \approx 5\%$ to $X[H] \approx 20\%$ and that it remains at a similar level when $X[H]$ is further increased to 30%; a monotonic decrease in Beryllium emission is simultaneously observed. The radiated power drops by a factor of 2 and reaches a minimum at $X[H] \approx 20\%$. It is discussed that poor single pass absorption at too high minority concentrations ultimately tailors the avoidance of the RF induced impurity influx. The edge density being different for different minority concentrations, it is argued that the impact ICRH has on the fate of heavy ions is not only a result of core (wave and transport) physics but also of edge dynamics and fueling.

1. INTRODUCTION

Carbon is not compatible with the long term use required for plasma facing components in future fusion reactors of the tokamak type e.g. from the point of view of erosion and tritium retention. W and Be were chosen as plasma facing materials for ITER. JET was equipped with beryllium (as opposed to C or C-coated) walls in the shutdown of 2010-2011. To sustain the very high heat loads inevitably falling on it and thus excluding the use of metals with a low melting point such as Be and in spite of the fact that its radiation is significant because of its large Z, a Tungsten (W) or Wcoated divertor was simultaneously installed. The recent JET campaign has focused on characterizing high density high temperature operation with this “ITER-like” wall (ILW). This paper briefly reports on two related aspects of the present understanding of ion cyclotron resonance heating (ICRH) or radio frequency (RF) heating in presence of the ILW: ICRH-specific impurity influx and heating performance. Complementing related discussions can be found in [1-6].

2. EXPERIMENTAL FINDINGS

The minority concentration is one of the most critical parameters that influence the heating efficiency in a minority heating scheme. Dedicated experiments aimed at changing the concentration $X[H]$ and studying its impact on impurities, radiation and heating efficiency were done; see Fig.1. The adopted ICRH scheme was minority hydrogen (H) fundamental cyclotron heating in a deuterium (D) majority plasma, a heating scenario typically guaranteeing good single-pass absorption. By operating at 42MHz and $B_0 = 2.7T$ while keeping the concentration low, efficient core heating with on-axis absorption was ensured. A central temperature increase of 0.5keV / MW was characteristic

for on-axis, and 0.3keV/MW for off-axis heating. These numbers are lower than what was realized with the C wall (DT up to 1keV/MW) but the change in energy content (Section 1 0:2MJ=MW) is similar; the density at which the recent experiments were done was typically higher (line integrated density around $6-7 \times 10^{19} \text{ m}^{-2}$ as opposed to $\approx 4-5 \times 10^{19} \text{ m}^{-2}$). Scanning the H concentration from modest values up to 30% reveals that the bulk radiation decreases steadily as a function of X[H] and reaches a minimum around 20% (see Fig.1-b); similar minima are observed in the Ni–XVIII and Fe–XVII signals while high ionization states (such as Ni–XXVI and Fe–XXV) show little X[H] dependence. The radiation increases again when proceeding to higher X[H] values. Scanning X[H] from 10 to 20%, the W concentration from Wquasi-continuum emission (Fig.1-c) [7] drops from 1.8×10^{-4} to 0.4×10^{-4} ; the W concentration deduced from W line emission - which yields concentrations closer to the core - follows the same trend, be it less pronounced. The Be-III emission - which characterizes the Be influx - drops by a factor 2 in the X[H] range considered. As can be seen in Fig.1-a depicting the plasma energy, the reduction in net heating efficiency is modest when keeping X[H] around 15% compared to the more commonly used X[H] $\approx 5\%$.

The increase of the radiation at very high X[H] is thought to be a consequence of the fact that the heating efficiency then has dropped significantly so that the RF electric field needs to grow large - giving rise to more efficient (usually non-resonant) particle acceleration in the edge - to ensure the launched power is damped inside the all-metal (Faraday cage) vessel. As demonstrated in Fig. 2, minority heating is most efficient at low concentrations. The plot shows the experimental heating efficiency as inferred from the thermal plasma energy via break-in-slope analysis and the theoretical prediction by the 1D TOMCAT code [8] adopting the density and temperature profiles of the experiment. Theoretically estimated absorptions of 80% of the launched power in a single full transit over the plasma at the smaller concentrations are observed, falling to a modest 20% at the highest minority concentrations reached. Parasitic losses away from the core, and in particular in the edge, cause deviations from the theoretically obtained result which assumes edge losses are absent. A loss of 25% of the power upon a full transit (double crossing) over the edge region allows to reconcile the theoretical estimates for single transit with the experimental (all transit) findings. The minority tail energy drops by a factor of 3 from about 240 to 80keV when doubling the H concentration from 10 to 20%. The reduction in heating efficiency has an immediate consequence for the ICRH launching system since the power fraction re-incident on the plasma edge is varying by a factor of 3 from 20% to 60% when scanning the minority concentration.

3. A TENTATIVE INTERPRETATION

In view of the fact that a strong correlation between the W source and the edge density [2] was experimentally observed and that increased impurity release is often associated with RF sheaths, it seems useful to explore the link between X[H] and the electric field magnitude near the antenna. This was done using a simple fast-wave-only evaluation accounting for the actual density profile. The adopted sheath-based philosophy is that mechanisms that enhance/reduce the edge electric field

amplitudes are candidates for explaining the increase/reduction of impurity release from the wall. The right subplot of Fig. 2 shows the edge density for a set of shots at different X[H]. The equation solved is $d^2 E_{\text{pol}} = dR^2 + k_{\perp, \text{FW}}^2(R) E_{\text{pol}} = 0$ in which E_{pol} is the poloidal RF electric field component, R the major radius and $k_{\perp, \text{FW}}^2$ the fast wave dispersion equation root for a specified parallel wave number, k_{\parallel} . Although this single mode 1D model lacks many ingredients of a fully trustworthy simulation, it can give first indications on the governing physics. The equation is solved for both the independent solutions, representing the antenna as a current density sheet situated between the metallic back wall of the antenna box and the main plasma, and can then be combined to any solution of the differential equation. Limiting oneself to the purely outgoing wave solution is aligned with what is traditionally done in antenna modeling assuming good single pass absorption is ensured. Allowing for a finite, complex (physically relevant) reflection coefficient permits to assess the impact of partial absorption of the waves for a prescribed power launched.

For purely outgoing waves but accounting for the experimentally observed change of the density profile, the model predicts a reduction of the electric field amplitude when going from X[H] \approx 10% to \approx 30%. The reductions are modest, maximally \approx 20% for the field amplitude and \approx 30% for the flux. Accounting for the reflection estimated by the TOMCAT code, the edge model on the contrary predicts that at X[H] = 30% an increase of the electric field strength by a factor 1.5–2 compared to the values reached for X[H] = 10% is required to ensure the same amount of power can be coupled. The impact of the modification of the edge (which e.g. shifts the fast wave cutoff point further outwards by 0.02m from $R = 3.87\text{m}$ to 3.89m for $k_{\parallel} = 6\text{m}^{-1}$) is significantly smaller than that when also accounting for the power re-incident on the edge. But this non-intentional edge density increase from the gas puffed to increase X[H] allows a coupling benefit that is aligned with the change in antenna resistance. The term 'coupling' used here relates the launched (active) power to the square of the poloidal electric field amplitude at the antenna, $P_{\text{launched}} = C_{\text{ant}} |E_{\text{pol}}|^2$ in a way similar to how the antenna resistance R_{ant} links the power to the square of the current I on the antenna straps, $P_{\text{launched}} = R_{\text{ant}} |I|^2$. The predicted increase of C_{ant} to 1.5 times its value when going from low to high X[H] is indeed crudely consistent with the corresponding increase of the experimentally found coupling resistance. Although the magnitude of the main beneficial effect (the fact that the core impurity level drops significantly when increasing X[H] to values of 15%) remains unexplained by the just mentioned simulations, the modeling suggests that a competition between two mechanisms may be at play when increasing the H concentration by gas puffing. One mechanism (related to incomplete single pass absorption) tends to enhance the edge electric field amplitude as well as plasma-wall interaction all around the machine while the other (gas injection to increase the H concentration which parasitically also increases the density in the edge) tends to reduce the edge electric field amplitude near the antenna. Following this line of reasoning, the initial decrease of X[W] and other impurity related signals may be interpreted a consequence of the improved coupling due to the modified edge density profile, while the opposite trend at higher X[H] can be seen as a consequence of the poor single pass absorption.

Although the competition of 2 opposing effects allows to qualitatively explain the experimental behavior, the relative magnitude of the 2 effects is improperly judged by the adopted 1D model, the predicted beneficial density effect being weaker than the detrimental effect of waves sloshing multiple times over the plasma and reflecting from the edge. A number of reasons can be given for that. First of all, the fact that various diagnostic signals are line integrals and that they depend on the density and temperature along their path, or that the information they provide is not at the antenna location but – at best – at a location magnetically connected to it (the available edge data being a typical example, and the coupling being a sensitive function of the edge density), puts an error bar on the adopted signals and the results inferred from them. Further more, the shots at small and high concentration have fairly different characteristics, likely directly or indirectly related to the different physics: At low concentration, minority heating efficiently heats the plasma so that much higher temperatures are reached; $T_{e,0} = 3.5\text{keV}$ when $X[\text{H}] \approx 10\%$ while it is only 1.5keV when $X[\text{H}] \approx 30\%$. At modest $X[\text{H}]$ sawtoothing causes electron temperature variations of 2keV , while at higher $X[\text{H}]$ sawtoothing is insignificant. The vast amount of energy that is evacuated from the core and transferred to the outer regions of the plasma due to sawtooth activity may contribute indirectly to enhanced sputtering. The highest energy particles that ICRH creates exhibit fat orbits that are prone to being unconfined and lost, hitting plasma facing components in the process. More generally, energy and particle transport differ when $X[\text{H}]$ - and thus the heating efficiency - changes. At low $X[\text{H}]$, the plasma tends to be in the medium confinement “M”-mode [9]. Also, it is useful to remind that the antenna spectrum is not composed of a single k_{\parallel} value. Whereas in dipole phasing - the phasing adopted for the experiments - most of the power is launched with $k_{\parallel} \approx 6\text{m}^{-1}$, the absorption efficiency of the waves is a sensitive factor of the parallel wave number. Low k_{\parallel} generally yields reduced heating efficiency and thus increased reflected power. On the other hand, low k_{\parallel} modes are less deeply evanescent in the plasma outer regions and thus are more easily coupled to the plasma. At high k_{\parallel} the opposite is the case. Since - in particular when the absorption is poor - the plasma significantly deforms the antenna spectrum because of the finite poloidal magnetic field, a 1D model is incapable of grasping the full complexity of the wave dynamics. Finally, a full spectrum of ill-absorbed waves reflect poloidally and toroidally from the vessel wall all around the machine, while well absorbed waves remain confined to the region in front of the antenna. Hence the ‘effective surface’ where sheath effects can act for a given field magnitude is different. Either way, the mere drop of the W high Z impurity concentration by more than a factor of 4 is an asset in an all-metal machine which justifies continued experimentation in the future. Getting a clearer view on the interplay between ICRH minority heating and gas puffing on the one hand, and impurity dynamics, radiation and sheath dynamics on the other is a necessity for successful use of ICRH in all-metal machines.

CONCLUSIONS

The recent JET experimental campaign showed that for all currently attained ICRH power levels

($P_{ICRH} \leq 4.5\text{MW}$), phasings and plasma configurations tested, the ILW and ICRH heating are compatible in L-mode as heat loads and impurity levels stay within acceptable limits without compromising the heating performance (see [1-6] for more details). Along with a strong reduction in the W level observed when the edge density is increased, it is found that it is beneficial to work at minority concentration of X[H] Section 1 15% - somewhat higher X[H] than those traditionally used for minority heating - to reduce the W concentration and bulk radiation. Various impurity related quantities reach a minimum at this intermediate X[H]. A tentative explanation for the observations has been proposed: Increasing X[H] on the one hand increases the edge density, which reduces the magnitude of the edge RF electric fields. But it also diminishes the absorption efficiency which increases the power fraction re-incident on the edge, the latter enhancing the RF electric fields throughout the machine and leading to increased plasma wall interaction; a similar behavior was observed in carbon wall experiments when studying the performance of low absorption scenarios (see e.g. [10]). Although the 2 opposing trends are observed and allow to explain the observed competition, the relative magnitude of the former with respect to the latter as inferred from experimental data and simple modeling suggests that other ingredients contribute to the observed phenomena.

REFERENCES

- [1]. P. Jacquet et al., Journal of Nuclear Materials **438** (2013) S379-S383
- [2]. V. Bobkov et al., Journal of Nuclear Materials **438** (2013) S160-S165
- [3]. M.-L. Mayoral et al., “Comparison of ICRF and NBI heated plasmas performance in the JET ITER-like wall”, this conference
- [4]. E. Lerche et al., “Statistical comparison of ICRF and NBI heating performance in JET-ILW L-mode plasmas”, this conference
- [5]. P. Jacquet et al., “ICRH heating in JET during initial operations with the ITER-like wall”, this conference
- [6]. A. Czarnecka et al., “Spectroscopic investigation of heavy impurity behavior during ICRH with the JET ITER-like wall”, this conference
- [7]. T. Pütterich et al., Plasma Physics and Controlled Fusion **50** (2008) 085016
- [8]. D. Van Eester & R. Koch, Plasma Physics and Controlled Fusion **40** (1998) 1949
- [9]. E.R. Solano et al., M-mode: axi-symmetric magnetic oscillation and ELM-less H-mode in JET, 40th EPS conference on Plasma Physics, Espoo, Finland
- [10]. E. Lerche et al., Plasma Physics and Controlled Fusion **54** 7(2012) 74008-74032

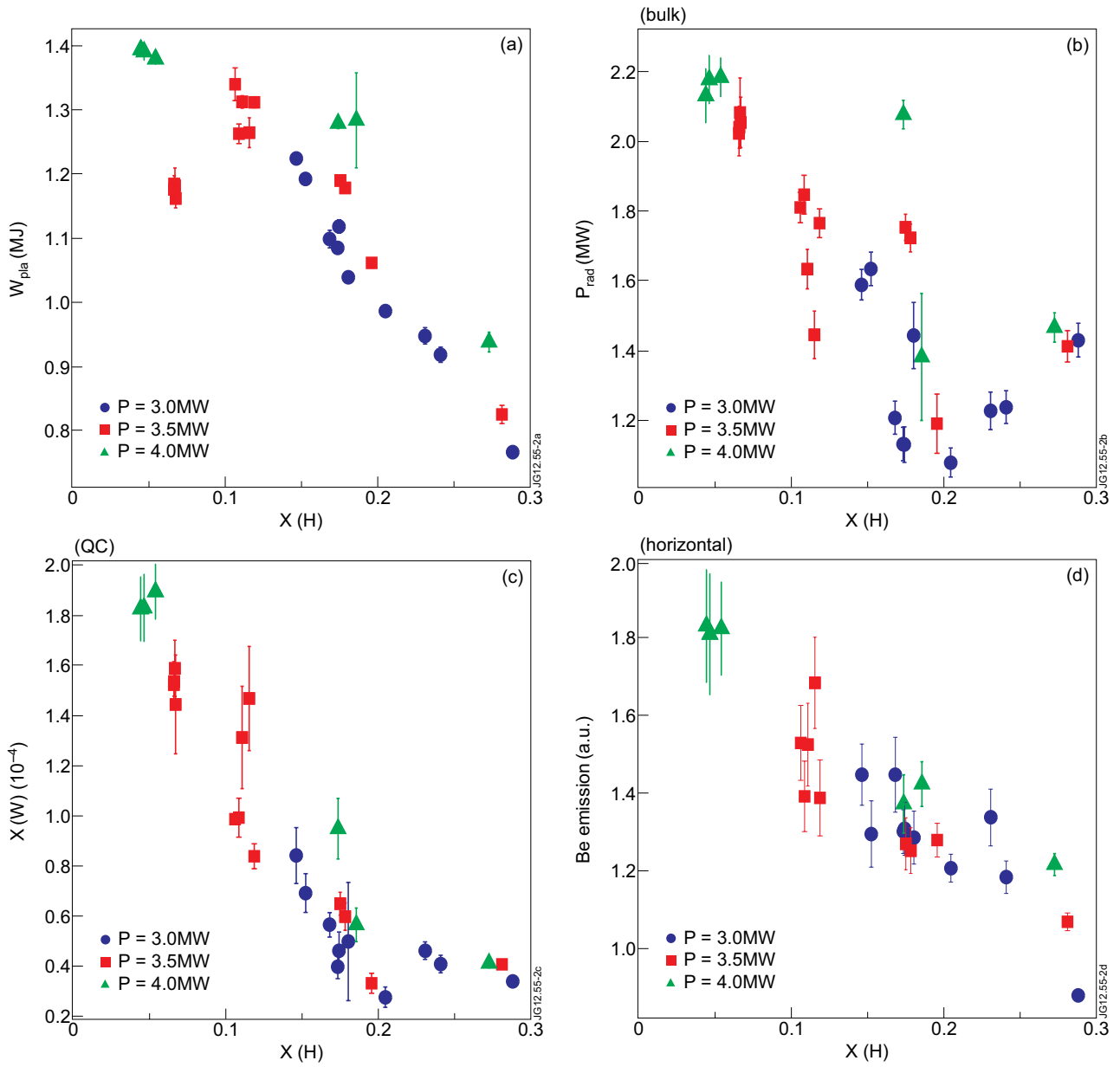


Figure 1: Plasma energy, radiated power, W concentration and Be emission as a function of the H concentration.

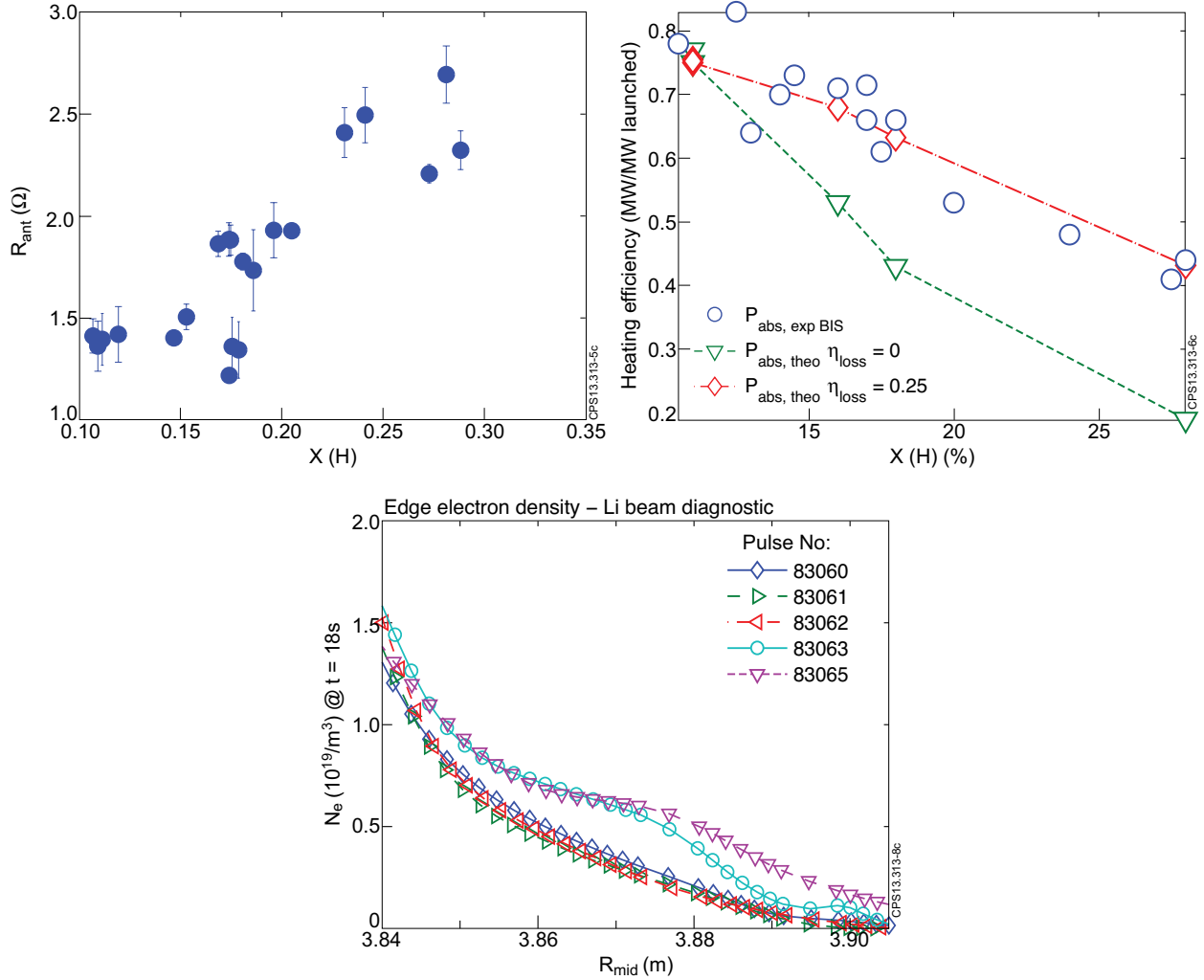


Figure 2: Experimental (dots) and theoretical (triangles: no loss; diamonds: 25% loss) heating efficiency, coupling resistance of antenna C of the JETA2 antennas (top right) and edge electron density at $t = 18\text{s}$ (bottom); $X[H]$ Section 1 0.11, 0.11, 0.16, 0.18 and 0.28, respectively for the respective shots.